molecular pharmaceutics

articles

Biophysical and Stabilization Studies of the *Chlamydia trachomatis* Mouse Pneumonitis Major Outer Membrane Protein

Sumin Cai,[†,‡] Feng He,[†,§] Hardeep S. Samra,[†,||] Luis M. de la Maza,[⊥] Maria E. Bottazzi,[#] Sangeeta B. Joshi,[†] and C. Russell Middaugh*[,†]

Laboratory for Macromolecular and Vaccine Stabilization, Department of Pharmaceutical Chemistry, University of Kansas, Lawrence, Kansas 66047, Department of Pathology and Laboratory Medicine, University of California Irvine, Irvine, California 92697-4800, and Department of Microbiology, Immunology, and Tropical Medicine, George Washington University Medical Center, Washington, D.C. 20037

Received April 27, 2009; Revised Manuscript Received July 27, 2009; Accepted August 3, 2009

Abstract: Native *Chlamydia trachomatis* mouse pneumonitis major outer membrane protein (nMOMP) induces effective protection against genital infection in a mouse challenge model. The conformation of nMOMP is crucial to confer this protective immunity. To achieve a better understanding of the conformational behavior and stability of nMOMP, a number of spectroscopic techniques are employed to characterize the secondary structure (circular dichroism), tertiary structure (intrinsic fluorescence) and aggregation properties (static light scattering and optical density) as a function of pH (3−8) and temperature (10−87.5 °C). The data are summarized in an empirical phase diagram (EPD) which demonstrates that the thermal stability of nMOMP is strongly pH-dependent. Three distinctive regions are seen in the EPD. Below the major thermal transition regions, nMOMP remains in its native conformation over the pH range of 3−8. Above the thermal transitions, nMOMP appears in two different structurally altered states; one at pH 3−5 and the other at pH 6−8. The EPD shows that the highest thermal transition point (∼65 °C) of nMOMP is near pH 6. Several potential excipients such as arginine, sodium citrate, Brij 35, sucrose and guanidine are also selected to evaluate their effects on the stability of nMOMP. These particular compounds increase the aggregation onset temperature of nMOMP by more than 10°C, without affecting its secondary and tertiary structure. These results should help formulate a vaccine using a recombinant MOMP.

Keywords: Chlamydia; MOMP; biophysical characterization; stabilization

Introduction

Chlamydia trachomatis is the most prevalent sexually transmitted bacterial pathogen.[1−3] It is estimated that 100 million new infections occur every year with a high proportion of them affecting young, sexually active individuals. In the United States, 3−4 million new cases of *C. trachomatis* infection occur annually. In females, cervicitis and urethritis

* To whom correspondence should be addressed: Department of Pharmaceutical Chemistry, University of Kansas, 2030 Becker Dr., Lawrence, KS 66047. Tel: (785) 864-5813. Fax: (785) 864-5814. E-mail: Middaugh@ku.edu.

† University of Kansas.

‡ Present address: VaxInnate Inc., Cranbury, NJ 08512.

§ Present address: Amgen Inc., Seattle, WA 98119.

|| Present address: MedImmune Inc., Mountain View, CA 94043.

⊥ University of California Irvine.

George Washington University Medical Center.

(1) Adler, M. W. Sexual health—health of the nation. *Sex. Transm. Infect.* **2003**, *79* (2), 85–7.

(2) LaMontagne, D. S.; Fine, D. N.; Marrazzo, J. M. Chlamydia trachomatis infection in asymptomatic men. *Am. J. Prev. Med.* **2003**, *24* (1), 36–42.

(3) Miller, W. C.; Ford, C. A.; Morris, M.; Handcock, M. S.; Schmitz, J. L.; Hobbs, M. M.; Cohen, M. S.; Harris, K. M.; Udry, J. R. Prevalence of chlamydial and gonococcal infections among young adults in the United States. *J. Am. Med. Assoc.* **2004**, *291* (18), 2229–36.

10.1021/mp900110q CCC: $40.75 © 2009 American Chemical Society
Published on Web 08/03/2009

are the most common acute manifestations. Their long-term sequelae include pelvic inflammatory disease, chronic abdominal pain, ectopic pregnancy and infertility.[4] In males, urethritis is the most frequent clinical presentation.[2] In newborns under six months of age, *C. trachomatis* is the most common cause of pneumonia and conjunctivitis. In addition, in countries with limited sanitary resources, trachoma, which is an eye disease and the leading cause of preventable blindness, and lymphogranuloma venereum (LGV), which may lead to severe systemic complications, are frequent clinical presentations of *C. trachomatis* infections.[5]

Efforts to vaccinate individuals against trachoma were initiated several decades ago.[6] Humans and monkeys were immunized with live or inactivated whole organisms. Although no vaccination programs were implemented, several practical lessons were learned from these trials. Specifically, protection was found to be, for the most part, serovar specific and short-lived. In poorly protected individuals, re-exposure to *C. trachomatis* resulted in more severe disease than that observed in nonvaccinated controls. As a consequence of this possible risk of vaccine-related immunopathology, it was proposed that the development of a subunit vaccine would be a preferred alternative to avoid the potential harmful effects of preparations containing the whole organism. In the last five decades, as the role of *C. trachomatis* in sexually transmitted infections was elucidated, the main focus of vaccine development indeed has shifted to the identification of target candidates that would induce protection against genital infections.

Among the various vaccine candidates evaluated to protect against chlamydial infection, the major outer membrane protein (MOMP) has been the antigen more thoroughly tested. DNA sequencing of the MOMP from several *C. trachomatis* serovars showed that this protein has four variable and five constant structural domains.[7] Phylogenetic analysis of the nucleotide sequence of MOMP supported the immunological classification of *C. trachomatis* isolates into various serovars.[8] This immunological classification was based on the cross-reactivity among serum samples generated by inoculating mice with the various serovars. Two major complexes delineated C (including serovars C, J, H, I, A, K and L3) and B (encompassing serovars B, Ba, E, D, L1 and L2) as well as a B-related complex (G and F) were recognized.[9] This classification was further supported by protection studies using a mouse model.[9] Animals immunized with one serovar were subsequently protected against a challenge with the same or a serologically closely related isolate in the same complex, but not against a distantly related serovar.

Recently, a vaccine was formulated that was effective at controlling a genital infection and preventing infertility in a mouse model.[10] This vaccine was prepared by isolating the native *C. trachomatis* mouse pneumonitis (MoPn; also referred as *Chlamydia muridarum*) MOMP directly from the organism. Native MoPn MOMP (nMOMP) forms trimers that have a predominant β-sheet structure and functions as a porin.[11]

Formulation development of membrane-associated proteins is a major challenge. The conformation of MOMP plays a key role in the ability of this molecule to confer protective immunity.[10,12−14] In the current study, we provide a detailed biophysical characterization of nMOMP in solution to better understand its thermal stability, which is assessed using a number of spectroscopic techniques. The spectroscopic data are summarized in the form of an empirical phase diagram (EPD), a matrix-based method which provides a comprehensive view of protein stability.[15,16] The effect of several compounds on nMOMP thermal stability was also investigated. Such molecules provide a starting point for further formulation development. Furthermore, excipients that sta-

(4) Westrom, L.; Joesoef, R.; Reynolds, G.; Hagdu, A.; Thompson, S. E. Pelvic inflammatory disease and fertility. A cohort study of 1,844 women with laparoscopically verified disease and 657 control women with normal laparoscopic results. *Sex. Transm. Dis.* **1992**, *19* (4), 185–92.
(5) Polack, S.; Brooker, S.; Kuper, H.; Mariotti, S.; Mabey, D.; Foster, A. Mapping the global distribution of trachoma. *Bull. World Health Org.* **2005**, *83* (12), 913–9.
(6) Grayston, J. T.; Wang, S. P. The potential for vaccine against infection of the genital tract with Chlamydia trachomatis. *Sex. Transm. Dis.* **1978**, *5* (2), 73–7.
(7) Stephens, R. S.; Sanchez-Pescador, R.; Wagar, E. A.; Inouye, C.; Urdea, M. S. Diversity of Chlamydia trachomatis major outer membrane protein genes. *J. Bacteriol.* **1987**, *169* (9), 3879–85.
(8) Fitch, W. M.; Peterson, E. M.; de la Maza, L. M. Phylogenetic analysis of the outer-membrane-protein genes of Chlamydiae, and its implication for vaccine development. *Mol. Biol. Evol.* **1993**, *10* (4), 892–913.
(9) Wang, S. P.; Grayston, J. T. Classification of trachoma virus strains by protection of mice from toxic death. *J. Immunol.* **1963**, *90*, 849–56.
(10) Pal, S.; Peterson, E. M.; de la Maza, L. M. Vaccination with the Chlamydia trachomatis major outer membrane protein can elicit an immune response as protective as that resulting from inoculation with live bacteria. *Infect. Immun.* **2005**, *73* (12), 8153–60.
(11) Sun, G.; Pal, S.; Sarcon, A. K.; Kim, S.; Sugawara, E.; Nikaido, H.; Cocco, M. J.; Peterson, E. M.; de la Maza, L. M. Structural and functional analyses of the major outer membrane protein of Chlamydia trachomatis. *J. Bacteriol.* **2007**, *189* (17), 6222–35.
(12) Brunham, R. C.; Zhang, D. J.; Yang, X.; McClarty, G. M. The potential for vaccine development against chlamydial infection and disease. *J. Infect. Dis.* **2000**, *181* (Suppl 3:S), S538–43.
(13) Stephens, R. S. Chlamydial genomics and vaccine antigen discovery. *J. Infect. Dis.* **2000**, *181* (Suppl. 3:S), 521–3.
(14) Batteiger, B. E.; Rank, R. G.; Bavoil, P. M.; Soderberg, L. S. Partial protection against genital reinfection by immunization of guinea-pigs with isolated outer-membrane proteins of the chlamydial agent of guinea-pig inclusion conjunctivitis. *J. Gen. Microbiol.* **1993**, *139* (12), 2965–72.
(15) Fan, H.; Li, H.; Zhang, M.; Middaugh, C. R. Effects of solutes on empirical phase diagrams of human fibroblast growth factor 1. *J. Pharm. Sci.* **2007**, *96* (6), 1490–503.
(16) Nonoyama, A.; Laurence, J. S.; Garriques, L.; Qi, H.; Le, T.; Middaugh, C. R. A biophysical characterization of the peptide drug pramlintide (AC137) using empirical phase diagrams. *J. Pharm. Sci.* **2008**, *97* (7), 2552–67.

bilize MoPn nMOMP can be candidates for the stabilization of MOMP of other serovars, including humans.

Materials and Methods

Preparation of Native MoPn MOMP. The nMOMP (strain Nigg II; American Type Culture Collection (ATCC), Manassas, VA) was grown in McCoy cells.[17] The extraction and purification of MOMP were performed as previously described.[10] In brief, nMOMP was washed with PBS (pH 7.4) and treated with 25 μg/mL of DNase for 2 h at 4 °C. The preparation was centrifuged, and the pellet was extracted twice with 2% of (3-[(3-cholamidopropyl)-dimethylammonio]-L-propane sulfonate) (CHAPS; Anatrace, Maumee, OH), in 0.2 M phosphate buffer (pH 5.5) containing 1 mM phenylmethylsulfonyl fluoride (PMSF; Calbiochem, San Diego, CA), 1 mM EDTA and 100 mM dithiothreitol (DTT; Roche Diagnostic Corporation, Indianapolis, IN). The pellet was then extracted with 2% Anzergent 3-14 (*n*-tetradecyl-*N*,*N*-dimethyl-3-ammonio-1-propanesulfonate) (Z3-14; Anatrace) in the same buffer at 37 °C. To further purify the nMOMP the supernatant was applied to a 30 × 2 cm hydroxyapatite column (Bio-Gel HTP Gel; Bio-Rad Laboratories; Hercules, CA) equilibrated with 0.02 M phosphate buffer (pH 5.5) containing 0.1% Z3-14 and 1 mM each of EDTA, PMSF and DTT.[17] The nMOMP was eluted with a linear gradient from 0.02 to 0.5 M in the same buffer. The peak fractions were analyzed by SDS−polyacrylamide gel electrophoresis (PAGE) and identified by Western blot using the monoclonal antibody MoPn40 to nMOMP.[11] Mass spectrometry analysis[18] and N-terminal sequencing[10] of nMOMP both revealed the material used in this study manifested a purity of >99%. In addition, extraction of nMOMP requires the use of DTT. However, the disulfide bonds are not necessary to maintain the trimer's structure.[11] In this paper a homogeneous form (trimer form) of nMOMP was characterized.

Purified nMOMP was dialyzed overnight at 4 °C against a series of 20 mM citrate−phosphate buffers (I = 0.1) containing 0.05% (w/v) Zwittergent 3-14 at pH 3−8 at one unit increments. Dialysis was performed using 10 kDa molecular mass cutoff Slide-A-lyzer dialysis cassettes (Pierce, IL). The nMOMP was then concentrated via centrifugation at 1750*g* at 4 °C using 10 kDa NMWCO Amicon ultrafiltration concentrators (Millipore, Billerica, MA). Protein concentration was determined by measuring UV absorption at 280 nm using ε = 1.5 (mL mg^{-1} cm^{-1}).

Far-UV Circular Dichroism (CD) Spectroscopy. Samples of nMOMP (pH 3−8) were concentrated to 0.2 mg/mL and transferred to a sealed quartz cuvette of 0.1 cm path length. The CD signal was measured at a 20 nm/min scanning speed over the far-UV range of 260−190 nm using a Jasco J-810 spectropolarimeter (Great Dunmow, U.K.) equipped with a 6-position Peltier temperature controller. CD spectra were collected at 2.5 °C intervals from 10 to 87.5 °C and a 15 °C/h heating rate. The CD signal at 216 nm was extracted from the spectra and followed as a function of temperature. The results were plotted using *Sigma Plot 8.0*.

Intrinsic (Trp) Fluorescence Spectroscopy. The tryptophan fluorescence of nMOMP (0.1 mg/mL) was measured using a Photon Technology International (PTI) 814 spectrofluorometer (Lawrenceville, NJ) equipped with a 4-position turret that is Peltier-controlled. An excitation wavelength of 295 nm (>95% Trp emission) was employed with a 2 nm slit width while the emission signal was collected from 300 to 400 nm with a slit width of 2 nm. The fluorescence spectra were measured at 2.5 °C intervals over the temperature range of 10 to 87.5 °C with a step size of 1 nm and 1 s integration time. The wavelength position of maximum emission was determined using a polynomial derivative fitting method executed in *Origin 7.0* software. The transition midpoint, however, was difficult to determine at some pH values.

Static Light Scattering. The static light scattering intensity was measured simultaneously using a 1 nm slit width during the fluorescence experiments employing a second photomultiplier located 180° to the fluorescence detector. The scattering intensity at the excitation wavelength (295 nm) was followed as a function of temperature and plotted using *Sigma Plot 8.0* software.

Turbidity Measurements. The optical density at 350 nm (OD_{350}) was measured as a direct indication of solution turbidity in nMOMP samples (0.05 mg/mL) in a 1 cm path length quartz cuvette. OD_{350} was recorded using an Agilent 8453 diode-array spectrophotometer (Palo Alto, CA) while the temperature was increased from 10 to 87.5 at 2.5 °C increments and with a 5 min equilibration time. The results were plotted using *Sigma Plot 8.0*.

Empirical Phase Diagram (EPD). The EPD method was employed to summarize the data obtained from the biophysical measurements mentioned above. CD signal at 216 nm, intrinsic fluorescence maximum peak position, static light scattering intensity and OD_{350} were normalized within each data set and the resulting data were used to generate an EPD. Each block of color in the EPD represents the overall contribution from three elementary colors (red, green and blue) that correspond to the three largest eigenvalues at each temperature and pH, calculated from the normalized results.[19] A detailed description of this method is presented elsewhere.[15,16,19−24] Changes in EPD color usually indicate

(17) Caldwell, H. D.; Kromhout, J.; Schachter, J. Purification and characterization of the major outer membrane protein of Chlamydia trachomatis. *Infect. Immun.* **1981**, *31*, 1161–76.

(18) Yen, T.-Y.; Pal, S.; de la Maza, L. M. Characterization of the disulfide bonds and free cysteine residues of the Chlamydia trachomatis mouse pneumonitis major outer membrane protein. *Biochemistry* **2005**, *44* (16), 6250–6.

(19) Kueltzo, L. A.; Ersoy, B.; Ralston, J. P.; Middaugh, C. R. Derivative absorbance spectroscopy and protein phase diagrams as tools for comprehensive protein characterization: a bGCSF case study. *J. Pharm. Sci.* **2003**, *92* (9), 1805–20.

(20) Markham, A. P.; Birket, S. E.; Picking, W. D.; Picking, W. L.; Middaugh, C. R. pH sensitivity of type III secretion system tip proteins. *Proteins* **2008**, *71* (4), 1830–42.

conditions under which conformational transitions take place as detected by the experimental methods.

Excipient Studies. Several excipients were included in this study at the following concentrations: 0.3 M arginine; 0.1% (w/v) Brij 35; 0.3 M guanidine-HCl; 0.2 M sodium citrate and 20% (w/v) sucrose. The effects of excipients were assessed by monitoring OD_{350} of protein-excipient (0.05 mg/mL protein concentration) mixtures for 2 h at pH 5 and 60 °C. Conditions for this assay were identified from color changes in the EPD (see Results). In addition, intrinsic fluorescence as well as static light scattering measurements (as described above) of nMOMP (0.05 mg/mL) were employed in the presence of excipients over the temperature range of 10−87.5 °C to study stabilizer effect, and the temperature midpoint of the major transition in Trp fluorescence was determined using the sigmoidal fitting tool in *Origin 7.0* software. CD melting experiments of nMOMP (0.2 mg/mL) were performed only in the presence of Brij 35 and sucrose due to signal interference by the other excipients.

Results

Biophysical Characterization of nMOMP. In this study, far-UV CD and intrinsic fluorescence spectroscopy were employed to assess the thermal stability of the secondary and tertiary structures of nMOMP, respectively. CD spectra of nMOMP before and after the thermal melt are shown in Figure 1 for all pH values examined. The CD signal at 10 °C suggests that nMOMP contains primarily β secondary structure. The protein displays very little pH dependence in secondary structure composition at low temperature. When the temperature reaches 87.5 °C, a significant loss of CD signal is observed at pH 3−5. This might be due to the loss of secondary structure and/or the protein precipitation at higher temperatures. The nMOMP at pH 6−8, in drastic contrast, manifests increased negative ellipticities after the thermal melt. This could be due to an increased amount of aggregation in solution which gives rise to the formation of intermolecular β sheets. The CD signal at 216 nm was monitored as a function of temperature, and the result is shown in Figure 2. A transition is observed at pH 3 near 45 °C while a similar transition is present at pH 4 and 5 at a much higher temperature, 65 °C. The protein at pH 6 exhibits a downward transition (increase in negative ellipticity) in the CD signal near 60 °C, and as the pH increases to 7 and 8, a similar transition is located near 50 °C.

The intrinsic fluorescence of nMOMP was also measured under different pH and temperature conditions. The peak position of the tryptophan fluorescence emission was extracted using a polynomial-based method, and the results are shown in Figure 3 as a function of temperature. On the basis of peak position sensitivity to the polarity of their environment, the tryptophan residues appear to be relatively buried at low temperatures, manifesting a peak position between 326 and 330 nm. The peak wavelength increases slightly as pH increases, suggesting more solvent exposure at higher pH values. The peak position of all samples slowly increases as the temperature increases followed by a transition above 30 °C. In addition, samples at pH 3−5 show large error bars at high temperature. This presumably results from sample precipitation at higher temperatures which causes the sample to become more heterogeneous (see below). Note that the fluorescence changes occur at significantly lower temperature than those seen in the CD studies.

Static light scattering (Figure 4) measured during the intrinsic fluorescence experiments displays a strong pH dependent behavior. The nMOMP at pH 3 undergoes an abrupt increase in scattering intensity around 40 °C, followed by pH 4 at 45 °C, pH 5 near 55 °C and pH 6 near 60 °C. Samples at pH 7 and 8 exhibit only limited intensity changes in scattering compared to lower pH conditions. The order of transition onset temperature is further verified by OD_{350} measurements (shown in Figure 5). The increase in OD_{350} correlates well with the transitions revealed by static light scattering with one exception. At pH 6, no significant changes in OD_{350} are seen as the temperature increases. This exception is probably due to higher sensitivity of right-angle static light scattering than that of optical density measurements. The results obtained with light scattering and optical density measurements suggest the presence of particles with increasing sizes under thermal stress probably due to protein aggregation. This behavior appears to be strongly dependent on pH. Furthermore, at pH 3−5, nMOMP also precipitates, which is indicated by the sharp intensity decrease observed in both static light scattering and OD_{350} of high temperatures. On the other hand, nMOMP at pH 6−8 may form soluble aggregates as suggested by the more limited intensity increase.

The empirical phase diagram (EPD) approach has been demonstrated to be an efficient method with which to summarize large volumes of biophysical data and that can be used to describe conformational changes and association phenomena.[16,20,21] Thus, an EPD was constructed for nMOMP using data from the CD signal at 216 nm, the intrinsic fluorescence peak position, the static light scattering intensity and the OD_{350} changes. A color presentation of the resultant EPD is shown in Figure 6 over a pH−temperature plane. The brown-green area at low temperatures (below 40 °C) presumably corresponds to the conditions under which

(21) Harn, N.; Allan, C.; Oliver, C.; Middaugh, C. R. Highly concentrated monoclonal antibody solutions: direct analysis of physical structure and thermal stability. *J. Pharm. Sci.* **2007**, *96* (3), 532–46.

(22) Ausar, S. F.; Espina, M.; Brock, J.; Thyagarayapuran, N.; Repetto, R.; Khandke, L.; Middaugh, C. R. High-throughput screening of stabilizers for respiratory syncytial virus: identification of stabilizers and their effects on the conformational thermostability of viral particles. *Hum. Vaccines* **2007**, *3* (3), 94–103.

(23) Peek, L. J.; Brandau, D. T.; Jones, L. S.; Joshi, S. B.; Middaugh, C. R. A systematic approach to stabilizing EBA-175 RII-NG for use as a malaria vaccine. *Vaccine* **2006**, *24* (31−32), 5839–51.

(24) Salnikova, M. S.; Joshi, S. B.; Rytting, J. H.; Warny, M.; Middaugh, C. R. Physical characterization of clostridium difficile toxins and toxoids: effect of the formaldehyde crosslinking on thermal stability. *J. Pharm. Sci.* **2008**, *97* (9), 3735–52.

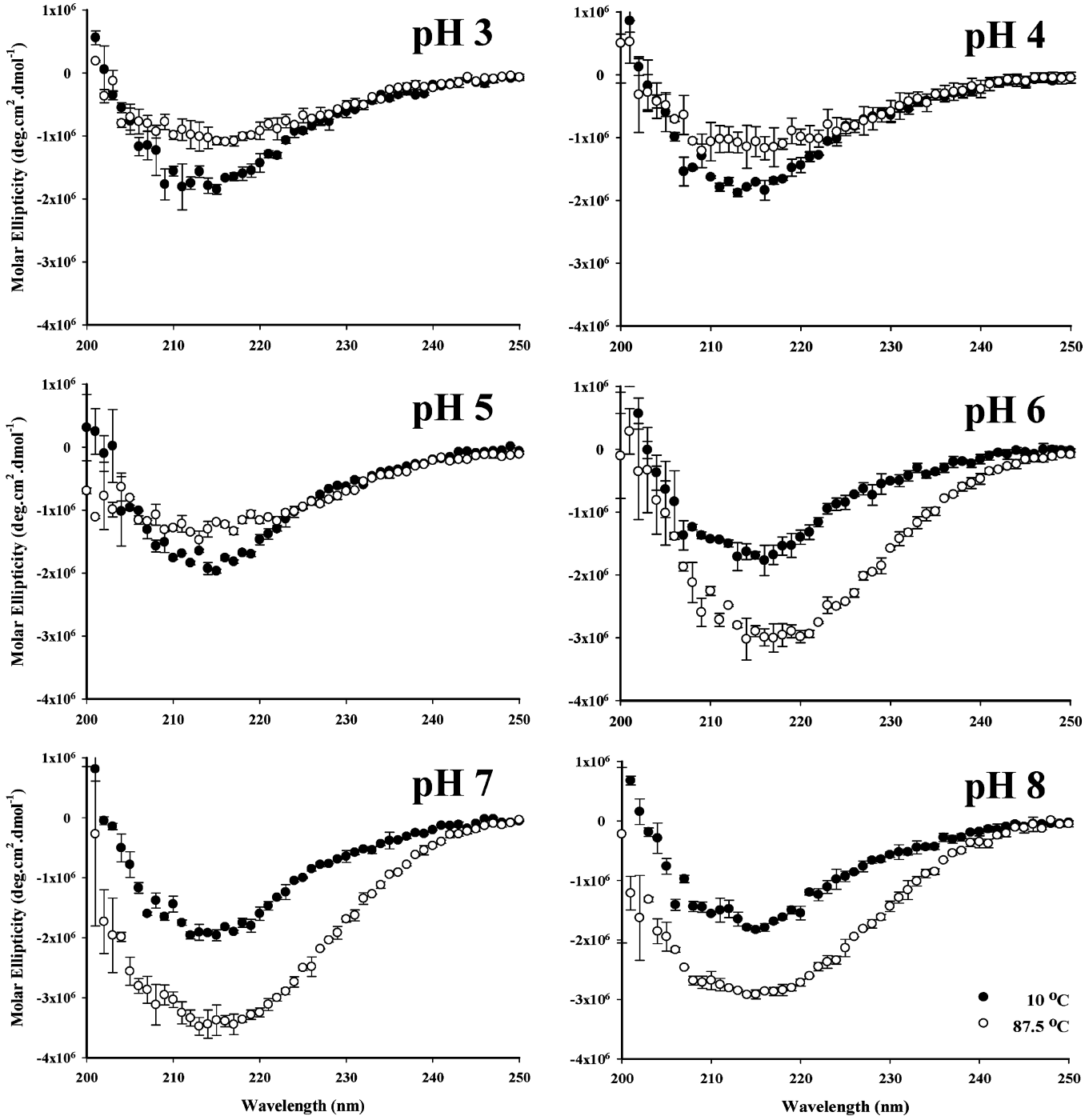

Figure 1. Secondary structure of nMOMP. Far-UV CD spectra (200−250 nm) were obtained for nMOMP at pH 3−8 (0.2 mg/mL). Scans at both the beginning (10 °C) and the end (87.5 °C) of the thermal melt are shown. The error bars were determined from duplicate measurements.

nMOMP exists in the native conformation. The upper left region of blue color indicates the protein structure is greatly altered at lower pH (3−5) and high temperatures. At pH 6−8, a transition "phase" exists between 40 and 60 °C where the color is slightly different from the area below. This suggests a partially unfolded structure of nMOMP. As the temperature increases at pH 6−8, nMOMP transforms into a structurally altered state (dark-red region on the upper right). A major application of EPDs is to reveal "stress" physical conditions (i.e., pH and temperature) that can cause significant structural changes in a protein and therefore may be used in the development of screening conditions for excipients.[22,23] After optimization, excipients identified using accelerated experimental approaches often sustain the protective effect in long-term storage scenarios.

Physical Stabilization. In a separate investigation, several excipients were identified to stabilize the native MOMP from *C. trachomatis* serovar A under elevated temperatures (Middaugh et al., unpublished result). Five representative compounds identified from these analyses were included in

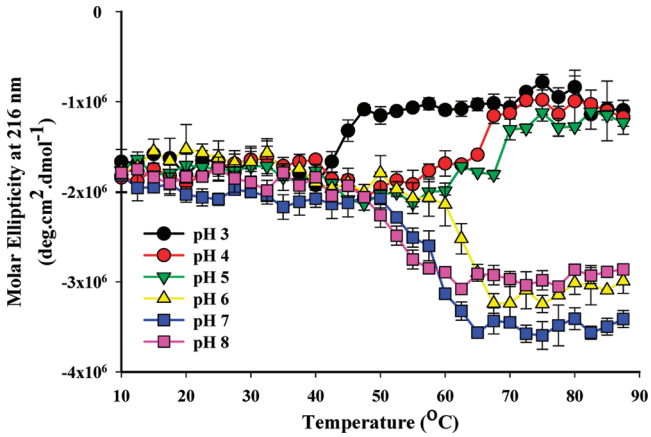

Figure 2. CD signal at 216 nm of nMOMP. The CD signal at 216 nm of nMOMP (0.2 mg/mL) is plotted as a function of temperature as an indication of secondary structure stability under thermal stress. Scans were obtained at 2.5 °C increments for duplicate samples (indicated by error bars).

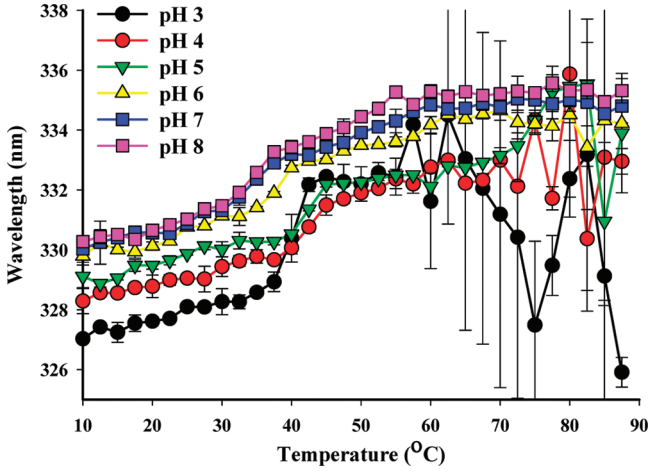

Figure 3. Intrinsic fluorescence of nMOMP. The intrinsic fluorescence peak position of nMOMP (0.1 mg/mL) is shown as temperature increases from 10 to 87.5 °C. All results were obtained from duplicate experiments.

the current study, and their effects on nMOMP structure stability were evaluated. Compounds chosen for further study were 0.3 M arginine, 0.1% (w/v) Brij 35, 0.3 M guanidine-HCl, 0.2 M sodium citrate and 20% (w/v) sucrose in a pH 5 citrate−phosphate buffer. Spectroscopic measurements as well as the more general EPD analysis reveal that nMOMP undergoes a "marked apparent phase transition" between 40 and 60 °C at pH 3−5. Since extreme low pH conditions are usually not preferred in pharmaceutical protein formulations, excipient studies of nMOMP were performed at pH 5. Therefore, nMOMP at pH 5 was incubated with selected excipients at 60 °C and the turbidity at OD_{350} was monitored for two hours (shown in Figure 7A). An OD increase of protein alone is triggered after 20 min of incubation and continues to progress. In contrast, the addition of the selected excipients to nMOMP stabilizes the OD at baseline level. Intrinsic fluorescence and static light scattering were also measured in the presence of the five compounds, and the

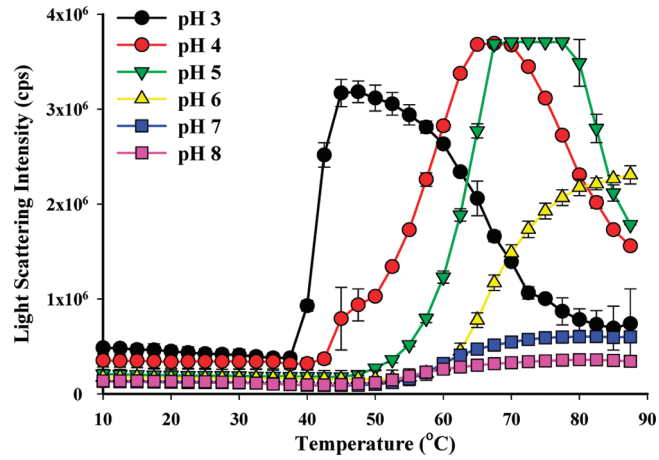

Figure 4. Static light scattering of nMOMP. The static light scattering intensity at 295 nm was recorded during the intrinsic fluorescence measurements of nMOMP (0.1 mg/mL). The intensity is shown as a function of temperature. The error bars indicate standard errors from duplicate measurements.

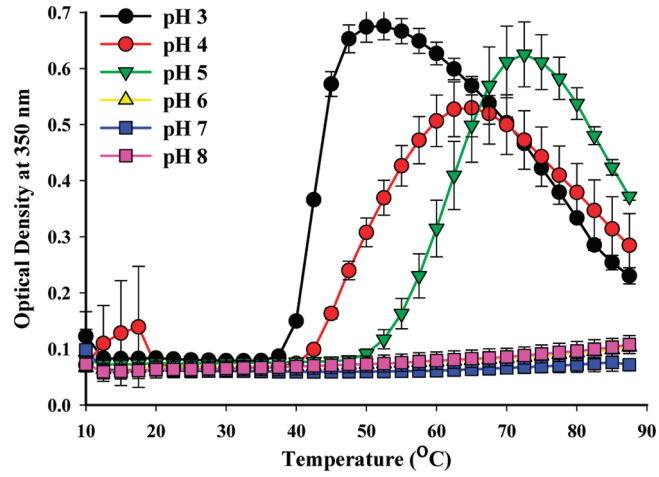

Figure 5. Turbidity measurement of nMOMP. The OD_{350} was monitored for nMOMP at 0.05 mg/mL. The increase in optical density is displayed as an indication of the formation of larger protein species (i.e., aggregates) when temperature increases. Standard errors from duplicates are presented in the form of error bars.

same heating rate was applied from 10 to 87.5 °C. A delay (of about 10 °C) is observed in the light scattering transition (Figure 7B) while the excipients show no significant effect on the intrinsic fluorescence emission transition midpoint (Table 1). Furthermore, two excipients (Brij 35 and sucrose) were incubated with nMOMP in a CD experiment at pH 5 and the results indicate no change in the thermal stability of the secondary structure (data not shown). Arginine, guanidine and sodium citrate interfere strongly with the CD absorption and were, therefore, excluded from this analysis.

Discussion

Biophysical methods have been widely employed to better understand the structural properties and to assess the stability

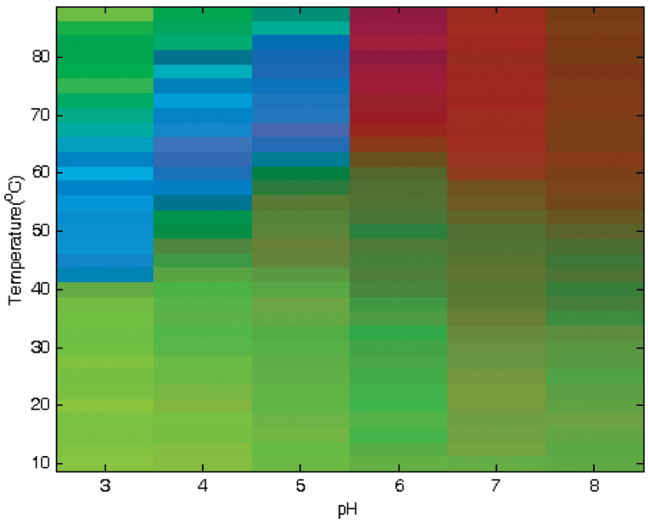

Figure 6. Empirical phase diagram (EPD) of nMOMP. The EPD of nMOMP was generated using an averaged CD signal at 216 nm, intrinsic fluorescence peak position, static light scattering intensity and OD_{350} measurement. Data were normalized within each technique, and the presence of changes in the spectroscopic measurements is manifested by color change in the EPD over the indicated pH (3−8) and temperature (10−87.5 °C) range. The coherent color distribution usually indicates the continuity of a particular physical state of the protein while conformational changes and associated/dissociation phenomena are seen as color changes.

of protein pharmaceuticals.[15,24] In this study, we employed a combination of methods including CD, intrinsic fluorescence, static light scattering and turbidity measurements to gain critical information concerning the stability of nMOMP, an important vaccine candidate. Together with these spectroscopic measurements, a wide range of pH and temperature conditions were applied to induce nMOMP structure changes. Earlier studies have shown the native conformation of the nMOMP to be a trimer containing predominately β-sheet structure with demonstrated function as a porin.[11] Other porins such as matrix porin (OmpF) and OmpL1 from Gram-negative bacteria have also been shown to have high β-strand contents.[25,26] CD experiments confirm that nMOMP is composed of predominately β sheet and that the secondary structure does not vary significantly over the pH range of 3 to 8 at low temperature. Marked differences in CD-detected nMOMP secondary structure stability, however, exist among the various pH conditions. The protein at pH 3 seems to be the least stable with an early CD signal loss near 45 °C while a similar event initiates above 60 °C at pH 4 and 5. As the pH increases to 6 or higher, a gain in negative ellipticity is

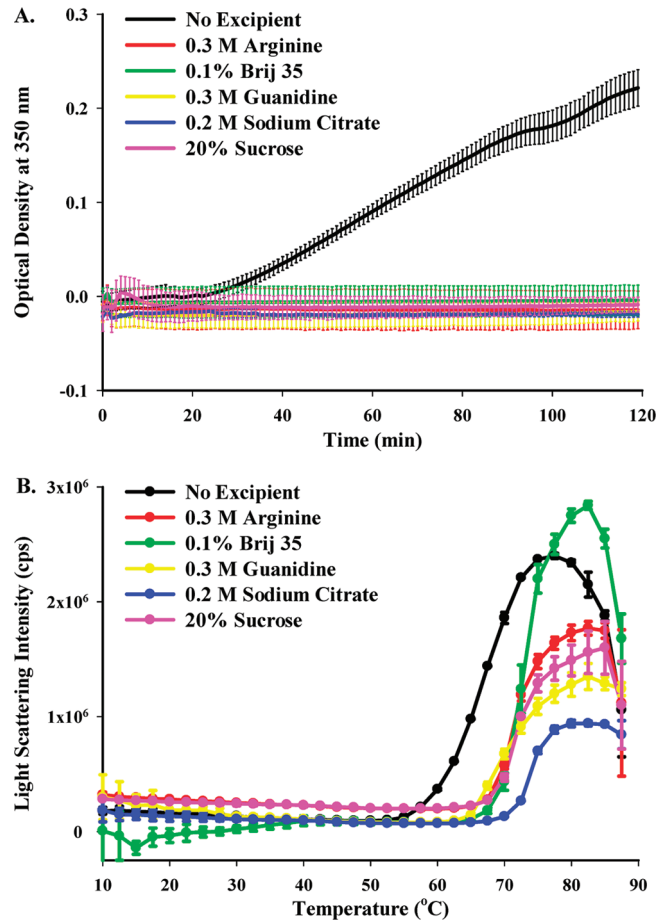

Figure 7. Effects of excipients on nMOMP stability. The nMOMP protein (0.05 mg/mL) at pH 5 was incubated at elevated temperature (60 °C) with five different excipients for two hours and the OD_{350} is shown in panel A from two independent experiments. The static light scattering results of nMOMP (0.05 mg/mL) in the presence of five excipient molecules are plotted against increasing temperature in panel B.

Table 1. Effects of Selected Compounds on the Stability of nMOMP Tertiary Structure

excipient[a]	transition midpoint (°C)[b]
none	42.4 ± 0.3
0.3 M arginine	42.0 ± 0.2
0.1% Brij 35	42.1 ± 0.7
0.3 M guanidine	41.0 ± 0.3
0.2 M sodium citrate	43.3 ± 0.2
20% sucrose	41.9 ± 0.3

[a] Excipients were added to 0.1 mg/mL nMOMP (pH 5) at indicated concentrations. Percentages are based on w/v ratio. [b] The intrinsic fluorescence was measured for nMOMP in the presence of excipients as a function of temperature from 10 to 87.5 °C. The midpoint of the thermally induced transition in fluorescence peak position was determined using the sigmoidal fitting tool in *Origin 7.0*. Calculated results are presented in the format of "average ± standard error".

observed at 50 °C. An increase in negative CD ellipticity between 215 and 220 nm is generally indicative of increased intermolecular β structure.[27,28] The tertiary structure as detected by intrinsic fluorescence changes of nMOMP starts

(25) Markovic-Housley, Z.; Garavito, R. Effect of temperature and low pH on structure and stability of matrix porin in micellar detergent solutions. *Biochim. Biophys. Acta* **1985**, *869* (2), 158–70.
(26) Shang, E.; Exner, M.; Summers, T.; Martinich, C.; Champion, C.; Hancock, R.; Haake, D. The rare outer membrane protein, OmpL1, of pathogenic Leptospira species is a heat-modifiable porin. *Infect. Immun.* **1995**, *63* (8), 3174–81.

to change significantly between 30 and 40 °C. Again the onset temperatures are pH-specific. Clearly, nMOMP manifests lower thermal transition points of its tertiary than its secondary structure over the pH range of 3−8, suggesting the existence of a partially unfolded conformation. The nMOMP first disrupts its tertiary structure and then loses secondary structure under thermal stress. The disruption of tertiary structure prior to secondary structure combined with aggregation is characteristic of the appearance of molten globule states.[29] Such intermediate states are not as commonly seen with membrane compared to soluble proteins. Both light scattering and optical density measurements were employed to assess the aggregation behavior of nMOMP. Both techniques reveal that the protein has a greater tendency to form larger species at pH 3−5 while only slight traces of associated proteins are observed in the right-angle light scattering experiments which are more sensitive than turbimetric measurements. All of the conformational events described above are well summarized in the nMOMP EPD over the experimental pH and temperature range examined.

Studies of the pH and thermal stability of native MOMP trimer performed by Sun et al. have shown the trimer to be stable in SDS between pH 5 and 8.[11] At pH 4 and 9, however, the trimer was partially dissociated and at pH 3 and 10 was completely dissociated.[11] In addition, the trimer was found to be stable from 4 to 37 °C.[11] At 45 °C, the trimer started to dissociate into monomers and completely dissociated following incubation at 65 °C.[11] These results were obtained, however, and analyzed by Western blotting.[11] Our results using different analytical techniques have found a similar thermal dependence of nMOMP. In contrast, no apparent pH dependence was observed at low temperatures. In addition, the CD and light scattering data in our studies show nMOMP to behave rather differently at pH 5 compared to pH 6−8 at high temperatures. We find that nMOMP is more stable in the pH range of 6−8 at temperature below 50 °C.

In this study, we selected five molecules that were identified as having stabilization effects on a native MOMP of a different serovar (data not shown). The choice of these particular excipients covers a wide range of molecule types. All five selections are shown to inhibit the aggregation of nMOMP by shifting the aggregation event to higher temperatures (∼10 °C difference). When incubated with nMOMP at 60 °C, these excipients are able to prevent the aggregation of the protein for at least up to 2 h. Although long-term storage studies have not been conducted, these excipients have the potential to further stabilize the protein at lower temperatures. Intrinsic fluorescence and CD experiments were repeated for nMOMP in the presence of these excipients. No significant stabilization was observed in either tertiary or secondary structure. This suggests that the mechanism of stabilization is not by protecting the native protein conformation from heat-induced structural change but rather by shielding the surface of the protein and interfering with protein−protein interactions. The precise mechanism by which the excipients inhibit the aggregation of proteins is in general not entirely clear. Stabilization of proteins by sugars, polyols and amino acids has been extensively studied and is thought in many cases to be due to nonspecific effects such as preferential hydration.[30−32] The presence of surfactants such as Brij 35 has been shown to prevent or reduce unfolding of proteins at liquid/air or liquid/solid interfaces.[33] In this case, the excipients prevent the aggregation but have no apparent effect on the structure or conformational stability of nMOMP, and the stabilization mechanism is probably due to direct binding of the excipients to the protein surface. One of the greatest challenges to the development of stable solution formulation of vaccines is to prevent aggregation over long periods under acceptable storage conditions (e.g., 2−8 °C). The stabilizers analyzed in this study demonstrate a striking ability to inhibit aggregation under thermal stress. These results thus provide a reasonable starting point for further formulation development of human vaccines.

Screening of potential excipients for protein pharmaceuticals is often performed using calorimetric techniques, such as differential scanning calorimetry (DSC). Upon identification based on increase in T_m determined by this method, excipients are subjected to optimization studies under normal storage conditions and in appropriate delivery devices. Although providing direct evidence of stabilization, DSC usually requires higher protein concentrations. Vaccines, however, are generally formulated at relatively low concentrations (e.g., 10−100 μg/mL). The spectroscopic measurements employed in this study provide analytical tools that can be used to assess excipient effects on protein samples at lower concentrations. Furthermore, the collection of physical methods employed here targets different physical properties of a protein, including secondary and tertiary structure changes as well as aggregation behavior. This permits the effects of the excipients to be better understood. We also demonstrated that information obtained from EPD analysis

(27) Kamerzell, T. J.; Unruh, J. R.; Johnson, C. K.; Middaugh, C. R. Conformational flexibility, hydration and state parameter fluctuations of fibroblast growth factor-10: effects of ligand binding. *Biochemistry* **2006**, *45* (51), 15288–300.

(28) Fan, H.; Vitharana, S. N.; Chen, T.; O'Keefe, D.; Middaugh, C. R. Effects of pH and polyanions on the thermal stability of fibroblast growth factor 20. *Mol. Pharmaceutics* **2007**, *4* (2), 232–40.

(29) Mach, H.; Ryan, J.; Burke, C.; Volkin, D.; Middaugh, C. Partially structured self-associating states of acidic fibroblast growth factor. *Biochemistry* **1993**, *32* (30), 7703–11.

(30) Lee, J.; Timasheff, S. The stabilization of proteins by sucrose. *J. Biol. Chem.* **1981**, *256* (14), 7193–201.

(31) Shimizu, S.; Smith, D. J. Preferential hydration and the exclusion of cosolvents from protein surfaces. *J. Chem. Phys.* **2004**, *121* (2), 1148–54.

(32) Uedaira, H.; Uedaira, H. Role of hydration of polyhydroxy compounds in biological systems. *Cell. Mol. Biol. (Noisy-le-grand)* **2001**, *47* (5), 823–9.

(33) Wang, Y. J. Parenteral Products pf Peptides and Proteins. In *Pharmaceutical Dosage Forms: Parenteral Medications*, 2nd ed.; Avis, K. E., Lieberman, H. A., Lachman, L., Eds.; Marcel Dekker Inc.: New York, 1992; Vol. 1, pp 283−319.

(i.e., apparent phase boundary conditions) can be used to develop robust assays to measure protein stabilization. Further evaluation of these excipients, however, requires additional efforts including chemical degradation and immunogenicity studies. Results obtained in this study concerning excipients can also be applied to the investigation of recombinant forms of MOMP which are more desirable candidates for actual vaccine production. The recombinant form of MOMP, like other membrane proteins, is extremely difficult to refold *in vitro* due to the tendency of the oligomeric protein to form insoluble aggregates and the presence of redox-sensitive cysteine residues. With the aid of appropriate excipients, however, it should be possible to extend the solubility of the protein and, subsequently, promote proper folding.

Acknowledgment. This work was supported by Public Health Service Grant AI-32248 from the National Institute of Allergy and Infectious Diseases.

MP900110Q